

# Guest-Driven Inflation of Self-Assembled Nanofibers through Hollow Channel Formation

Yanqiu Wang,<sup>†,||</sup> Zhegang Huang,<sup>‡,||</sup> Yongju Kim,<sup>\*,†</sup> Ying He,<sup>†</sup> and Myongsoo Lee<sup>\*,†</sup>

<sup>†</sup>State Key Lab for Supramolecular Structure and Materials, College of Chemistry, Jilin University, Changchun 130012, China

<sup>‡</sup>Department of Chemistry, Harbin Institute of Technology, Harbin150001, China

**S** Supporting Information

**ABSTRACT:** The highlight of self-assembly is the reversibility of various types of noncovalent interactions which leads to construct smart nanostructures with switchable pores. Here, we report the spontaneous formation of inflatable nanofibers through the formation of hollow internal channels triggered by guest encapsulation. The molecules that form this unique nanofibers consist of a bent-shaped aromatic segment connected by a *m*-pyridine unit and a hydrophilic dendron at its apex. The aromatic segments self-assemble into paired dimers which stack on top of one another to form thin nanofibers with pyridine-functionalized aromatic cores. Notably, the nanofibers reversibly inflate into helical tubules through the formation of hollow cavities triggered by *p*-phenylphenol, a hydrogen-bonding guest. The reversible inflation of the nanofibers arises from the packing rearrangements in the aromatic cores from transoid dimers to cisoid macrocycles driven by the reversible hydrogen-bonding interactions between the pyridine units of the aromatic cores and the *p*-phenylphenol guest molecules.

Spontaneous assembly of small molecular modules driven by the interplay of various noncovalent interactions is a challenging topic of the research in the field of supramolecular chemistry.<sup>1</sup> The reversibility of such noncovalent interactions opens up interesting applications to direct the systems toward the construction of smart materials with responsive functions.<sup>2</sup> Various responsive supramolecular structures can be formed by self-assembly of small block molecules based on rigid aromatic segments.<sup>3</sup> In contrast to conventional block copolymers and lipid amphiphiles, additional noncovalent interactions of the aromatic segments endow self-assembled structures with dynamic responsive properties without the collapse of their structural integrity. For example, macrobicycles grafted by hydrophilic oligoether dendrons aggregate to form porous sheets with gated lateral pores in response to external guests.<sup>4</sup> The aromatic guest molecules drive the gating motion of the pores by enhancing lateral aromatic interactions. Lateral attachment of the dendritic oligoether segments into an aromatic rod leads the molecules to self-assemble into foldable sheets that spontaneously roll-up into scrolled tubules upon heating.<sup>5</sup> The entropically driven dehydration of the oligoether chains triggers this structural change to reduce the dehydrated surface area that is exposed to water environments.

We have recently reported that breathing tubules with chirality inversion could be constructed by self-assembly of bent-shaped aromatic building blocks containing an oligoether dendron at its apex.<sup>6</sup> The bent-shaped rigid segments with an internal angle of 120° fit together easily to form hexameric macrocycles which endow the rings with flexible diameter through sliding motion between the molecules, creating the dynamic tubules. Self-assembled fiber structures are also able to respond to external stimuli by changing their shapes such as folded helices, ribbons, and tubules, which are mostly based on elementary nanofibers.<sup>2b</sup> Although numerous additional examples of responsive self-assembled structures have been reported,<sup>7</sup> inflation of closed nanostructures accompanied by creating hollow internal cavities is limited.<sup>8</sup>

We reported aromatic rod amphiphiles that self-assemble into uniform nanofibers in which the aromatic segments are paired as dimeric associations surrounded by hydrophilic chains.<sup>3e</sup> These observations led us to envision that a bent aromatic segment with an internal functional moiety would give rise to the formation of nanofibers with functionalized aromatic cores. The functional nanofibers would encapsulate guest molecules within their interiors through host–guest interactions, although the nano-objects are based on closed structures. This molecular recognition event would lead the closed nanostructures to inflate to provide additional space for the guest molecules. With this

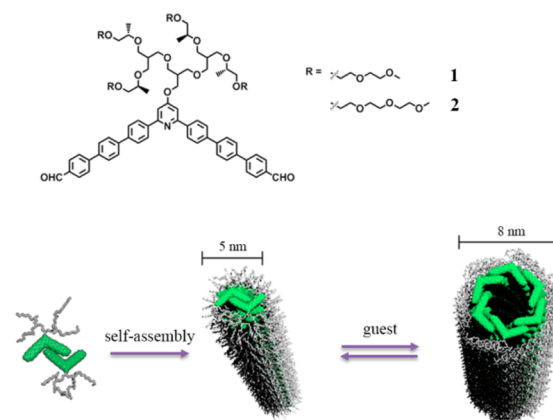


**Figure 1.** Molecular structures of bent-shaped rigid amphiphiles and schematic representation of inflation of a self-assembled nanofiber into a hollow tubule.

Received: October 3, 2014

Published: November 5, 2014

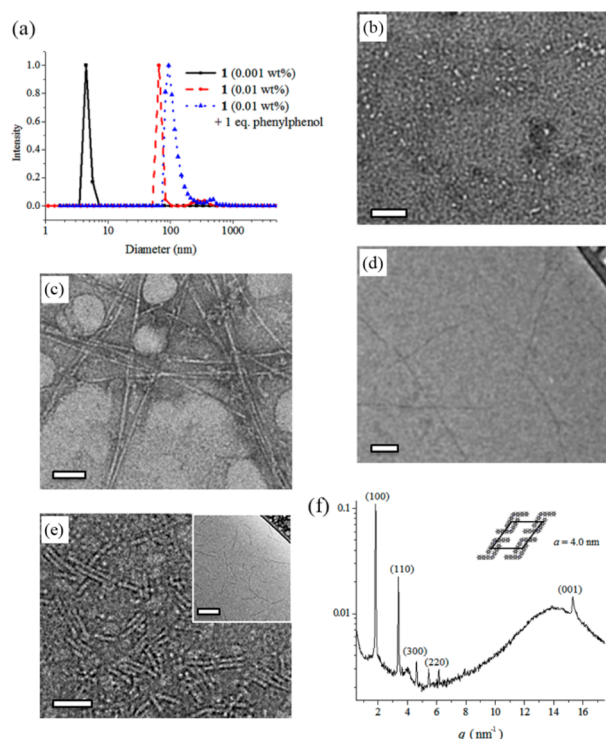


**Figure 2.** (a) Size distribution graph from DLS measurements: aqueous solution of **1** (0.001 wt %, black solid line), **1** (0.01 wt %, red dashed line), and **1** (0.01 wt %) in the presence of 1.0 equiv of phenylphenol (blue dotted line). (b) Negative-stain TEM image of **1** from a 0.001 wt % aqueous solution. (c) Negative-stain TEM image and (d) cryo-TEM image of a solution of **1** (0.01 wt %). (e) Negative-stain TEM image and cryo-TEM image (inset) of **2** from a 0.01 wt % aqueous solution. (f) XRD pattern of 2-D columnar structure performed on the films from fast evaporation of aqueous solution of **1**. All the scale bars are 50 nm.

idea in mind, we have synthesized self-assembling molecules consisting of a short bent-shaped aromatic segment containing a *m*-linked pyridine unit as a hydrogen-bonding acceptor and a hydrophilic oligoether dendron grafted at its apex.

We present here the closed nanofiber structures formed through self-assembly of the bent-shaped rigid amphiphiles that reversibly inflate into hollow tubules triggered by the guest addition (Figure 1). The self-assembling molecules that form the inflatable nanofiber structures consist of a short bent-shaped aromatic segment containing a *m*-pyridine unit at the inner position with a hydrophilic oligoether dendron at its apex. The synthesis of aromatic amphiphiles **1** and **2** was performed according to the procedures described previously.<sup>6,9</sup> The resulting molecules were characterized by <sup>1</sup>H- and <sup>13</sup>C NMR spectroscopies and MALDI-TOF mass spectroscopy were shown to be in full agreement with the structures presented.

To investigate the aggregation behavior of **1** and **2**, we have performed dynamic light scattering (DLS) experiments (Figures 2a and S2). The DLS data of the aggregates in diluted aqueous solutions (0.001 wt %) showed to be a hydrodynamic diameter of ~5 nm for both the molecules, indicative of the formation of small micellar aggregates in aqueous solution. The micellar structures of **1** and **2** were confirmed by using transmission electron microscopy (TEM) (Figures 2b and S3). When the samples were cast from the aqueous solution and then negatively stained with uranyl acetate, the images of both of the molecules showed spherical micelles with a uniform diameter of ~5 nm. This dimension in diameter is approximately twice the extended

molecular lengths (2.4 nm for **1** and 2.8 nm for **2**, respectively, from CPK modeling), suggesting that the aromatic segments are faced with each other in which the aromatic pairs are surrounded by hydrophilic dendrons (Figure 1).

With increasing the solution concentration, the length of the aggregates increases up to several hundreds of nanometer for **1** and several tens of nanometer for **2**, respectively, at the concentrations of 0.01 wt %. In contrast to the diluted solutions, TEM revealed that the solution of **1** showed thin nanofibers with a uniform diameter of about 5 nm and lengths with several hundreds of nanometer (Figure 2). The formation of nanofibers was further confirmed by using cryo-TEM with the vitrified solutions (Figure 2d). However, the nanofibers of **2** showed to be much shorter than those of **1** (Figure 2e), suggesting that the longer dendrimers lead to premature termination for nanofiber growth, most probably due to the greater steric repulsions between the larger dendritic segments. This result is consistent with those observed in the reported results.<sup>10</sup> The observed diameters of ~5 nm in the nanofibers indicate that the dimeric micelles stack on top of each other to form thin nanofibers surrounded by dendritic chains (Figure 1).

To corroborate the molecular arrangements of the aromatic segments within the nanofibers, X-ray diffraction (XRD) measurements were performed on the films prepared from fast evaporation of aqueous solution of **1** (Figure 2f). The diffraction pattern showed several sharp reflections corresponding to a 2-D columnar structure with a lattice parameter of 4.0 nm which is close to the diameter obtained from TEM results.<sup>11</sup> On the basis of X-ray results and density considerations, the number of molecules in a single slice of the columns could be estimated to be 2. This result further supports that the cross section of the single nanofiber consists of a paired aromatic segment. Circular dichroism (CD) spectra of the both of the solutions showed a weak Cotton effect in the spectral range of the aromatic segments (Figure 3b). Taken all data together, it can be considered that the nanofibers are based on the stacking of paired aromatic segments surrounded by hydrophilic dendrons (Figure 1).

The formation of nanofibers with pyridine functionalized aromatic core led us to investigate whether the nanofibers would encapsulate hydrophobic, hydrogen-bonding donor guest molecules such as phenylphenol, through both hydrogen-bonding and hydrophobic interactions.<sup>12</sup> We therefore investigated to encapsulate poorly water-soluble *p*-phenylphenol as a hydrogen-bonding donor within the nanofiber solutions (0.01 wt %) of **1**. Indeed, the nanofiber solution readily solubilized *p*-phenylphenol in aqueous solution with the preservation of their 1-D structures. Upon addition of phenylphenol to the aqueous solution of **1**, the absorption maximum centered at 325 nm is red-shifted up to 1.0 equiv, beyond which the absorption maximum did not change with noticeable precipitation upon further addition of the guest to the solution (Figure 3a). This result indicates that the maximum amount of phenylphenol loading per amphiphilic molecule is 1.0 equiv, implying that the phenylphenol guests form hydrogen bonds with the pyridine units of the aromatic segments. Indeed, Raman spectrum of the phenylphenol complex of **1** showed the strong band at 1601 cm<sup>-1</sup> associated with a hydrogen-bonded pyridine complex (Figure S5a),<sup>13</sup> demonstrating that the phenylphenol guests are encapsulated within the nanofiber interior through hydrogen-bonding interactions. Notably, the absorption maximum of **1** is red-shifted upon addition of the guest molecules, which is characteristic of *J*-type aggregates of chromophores.<sup>6b,14</sup> The solutions of **2** showed similar absorption behavior to those of **1**,

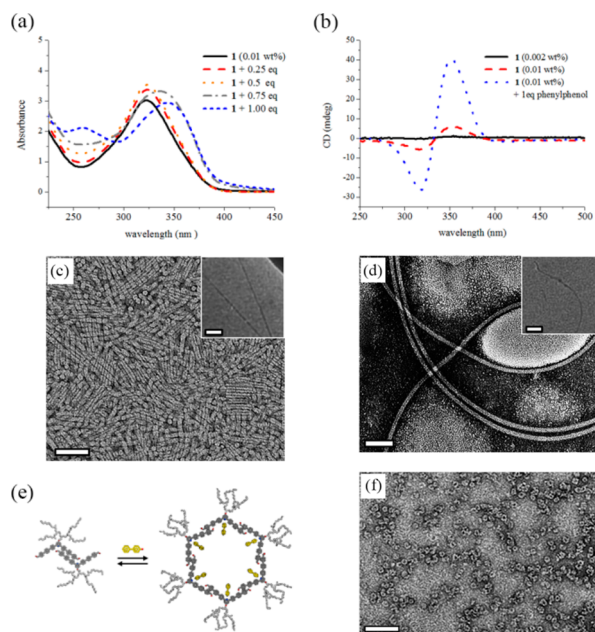


**Figure 3.** (a) Absorption spectra of aqueous solutions **1** (0.01 wt %) in the presence of different equiv of phenylphenol. (b) CD spectra of **1** from 0.002 wt % (black solid line), 0.01 wt % aqueous solution (red dashed line), and 0.01 wt % with 1.0 equiv of phenylphenol (blue dotted line). Negative-stain TEM image and cryo-TEM image (inset) from 0.01 wt % aqueous solution in the presence of 1.0 equiv of phenylphenol of (c) **1** and (d) **2**. (e) Schematic representation of the transformation between transoid dimer to cisoid macrocycle. (f) Negative-stain TEM image of a solution of **1** (0.002 wt %) with 1.0 equiv of phenylphenol. All the scale bars are 50 nm.

which showed to be a red-shifted absorption maximum upon addition of the guest molecules (Figure S7).

Remarkably, the phenylphenol guest triggers a significant increase in diameter of the nanofibers with enhanced chirality. Upon addition of phenylphenol, CD spectra of the both solutions showed a significant Cotton effect in the spectral range of the aromatic segments, in contrast to those of the solutions before guest addition (Figure 3b). Even after the addition of the guest molecules, the structural integrity of 1-D objects remained unchanged, which was visualized by TEM (Figure 3). However, the size of the nanofibers in external diameter showed to be significantly increased upon addition of guest molecules. When the samples were cast from the 0.1 equiv guest containing solutions of **1** (0.01 wt %), the images showed elongated objects with an external diameter of 8 nm (Figure 3c), demonstrating that the encapsulation of the guest molecules enforces the nanofibers to be swelling in diameter from 5 to 8 nm. Notably, the dried-TEM image showed a dark interior separated by two white lines, characteristic of tubular structures with hollow internal cavities.<sup>15</sup> These results demonstrate that the hydrogen-bonded guest triggers the thin nanofibers to inflate into tubular structures through the creation of the internal cavity along the fiber axis. This increase of the nanofibers in diameter was further confirmed by cryo-TEM with vitrified solutions (Figure 3c, inset). Similarly, the nanofibers of **2**, even though they are short in length before the addition of guest molecules, transform into long tubules accompanied by swelling in external diameter from 5 to 8 nm (Figure 3d). The CD spectra of the solutions of **2** also showed an increased Cotton effect upon addition of guest molecules (Figure S5b), indicating the more

closed helical stackings of the aromatic segments than those of the solutions in the absence of the guest molecules.

On the basis of these results, we propose the inflation mechanism of the nanofibers considering molecular rearrangements triggered by hydrogen-bonding interactions. The complexation of pyridine units with phenylphenol guest molecules would cause steric constraints at the inside of the aromatic cores. To relieve the steric repulsions without sacrificing  $\pi$ - $\pi$  stacking interactions, the overlapped aromatic pairs are slipped with each other to fit hydrogen-bonded guest molecules, as reflected in red-shifted absorption maximum.<sup>6,14</sup> To reduce hydrophobic surfaces of the slipped aromatic segments containing hydrophobic guest molecules which are exposed to water environments, the aromatic pairs containing hydrogen-bonded guests further assemble to form a curved macrocycle with hydrophilic chain exteriors through a conformational change from transoid to cisoid (Figure 3e). In the cyclic geometry, the hydrophobic guests would be surrounded more efficiently by the aromatic segments. The resulting macrocycles stack on top of one another with mutual rotation in the preferred direction to form a tubular structure with a one-handed helical sense, as reflected in a strong CD signals. To support this explanation, we have additionally performed TEM experiments with a diluted solution (0.002 wt %) of **1** containing 1.0 equiv of phenylphenol (Figure 3f). The image showed toroidal structures with an external diameter of  $\sim 8$  nm which is consistent with the tubular dimensions. This result indicates that the tubular structures are based on the stacks of noncovalent macrocycles formed through a guest trigger.

The guest-driven tubular structures showed to be collapsed into the original thin nanofibers upon the removal of the guest molecules, demonstrating that the inflation of the nanofibers is reversible depending on the presence of the guest molecules. When ammonium hydroxide was added to the guest containing solution of **1** (0.01 wt %), the tubules showed to be reconverted into the thin nanofibers ( $d = 4.5$  nm), which was confirmed by TEM (Figure 4a). The added ammonium hydroxide drives the hydrogen-bonded guests to liberate from the tubular cavities as a water-soluble phenolate form, which was confirmed by UV measurements (Figure 4b). Consequently, the removal of the guests by the addition of ammonium hydroxide leads the hollow tubules to be recovered into thin nanofibers through the molecular rearrangements of macrocycles into paired dimers.

In conclusion, we have demonstrated that amphiphilic molecules based on a bent-shaped aromatic segment containing

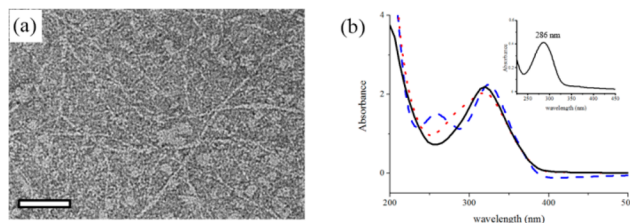


**Figure 4.** (a) Negative-stain TEM image of **1** from 0.01 wt % aqueous solution after the addition of 10 mM ammonium hydroxide solution. The scale bar is 50 nm. (b) Absorption spectra of **1** from 0.01 wt % solution (black solid line), 0.01 wt % solution containing phenylphenol (blue dashed line), and 0.01 wt % solution containing phenylphenol after treatment of 10 mM ammonium hydroxide solution (red dotted line). The inset is absorption spectra after subtracting the black solid line from the red dotted line, indicative of the phenolate formation.

*m*-linked pyridine self-assemble into closed dimeric micelles which stack to form thin nanofiber structures with a diameter of ~5 nm. The pyridine-functionalized nanofibers encapsulate *p*-phenylphenol guests through hydrogen-bonding interactions without compromising the shape integrity. Remarkably, the encapsulation of the guest molecules triggers the closed nanofibers to inflate into hollow tubules ( $d = \sim 8$  nm) through the molecular rearrangements of closed aromatic pairs into hollow hexameric macrocycles. As opposed to conventional host–guest chemistry,<sup>16</sup> the most notable feature of our systems is their ability to reversibly inflate closed systems into open structures triggered by guest molecules. Such a unique inflation phenomenon of self-assembled nanostructures provides the new insight of using self-assembly to construct an artificial virus containing double-stranded DNA inside through systematic cooperative interactions that mimic natural TMV virus.<sup>17</sup>

## ■ ASSOCIATED CONTENT

### Supporting Information

Experimental details and characterization data. This material is available free of charge via the Internet at <http://pubs.acs.org>.

## ■ AUTHOR INFORMATION

### Corresponding Authors

mslee@jlu.edu.cn

yjkim@jlu.edu.cn

### Author Contributions

<sup>†</sup>These authors contributed equally.

### Notes

The authors declare no competing financial interest.

## ■ ACKNOWLEDGMENTS

This work was supported by 111 Project (Grant B06009), NSFC (Grant 51473062), and 1000 program.

## ■ REFERENCES

- (1) (a) Aida, T.; Meijer, E. W.; Stupp, S. I. *Science* **2012**, *335*, 813. (b) De Greef, T. F. A.; Smulders, M. M. J.; Wolffs, M.; Schenning, A. P. H. J.; Sijbesma, R. P.; Meijer, E. W. *Chem. Rev.* **2009**, *109*, 5687. (c) Shimizu, T.; Masuda, M.; Minamikawa, H. *Chem. Rev.* **2005**, *105*, 1401. (d) Ajayaghosh, A.; Praveen, V. K. *Acc. Chem. Res.* **2007**, *40*, 644. (e) Rosen, B. M.; Wilson, C. J.; Wilson, D. A.; Peterca, M.; Imam, M. R.; Percec, V. *Chem. Rev.* **2009**, *109*, 6275.
- (2) (a) Yagai, S.; Kinoshita, T.; Kikkawa, Y.; Karatsu, T.; Kitamura, A.; Honsho, Y.; Seki, S. *Chem.—Eur. J.* **2009**, *15*, 9320. (b) Kim, H.-J.; Kim, T.; Lee, M. *Acc. Chem. Res.* **2010**, *44*, 72. (c) Shao, H.; Parquette, J. R. *Angew. Chem., Int. Ed.* **2009**, *48*, 2525. (d) Goto, H.; Furusho, Y.; Yashima, E. *J. Am. Chem. Soc.* **2007**, *129*, 109. (e) Gopal, A.; Hifisudheen, M.; Furumi, S.; Takeuchi, M.; Ajayaghosh, A. *Angew. Chem., Int. Ed.* **2012**, *51*, 10505. (f) Ajayaghosh, A.; Chithra, P.; Varghese, R. *Angew. Chem., Int. Ed.* **2007**, *46*, 230. (g) Yagai, S.; Kubota, S.; Saito, H.; Unoike, K.; Karatsu, T.; Kitamura, A.; Ajayaghosh, A.; Kanesato, M.; Kikkawa, Y. *J. Am. Chem. Soc.* **2009**, *131*, 5408. (h) Palmans, A. R. A.; Meijer, E. W. *Angew. Chem., Int. Ed.* **2007**, *46*, 8948. (i) Sim, S.; Kim, Y.; Kim, T.; Lim, S.; Lee, M. *J. Am. Chem. Soc.* **2012**, *134*, 20270. (j) Yan, Y.; Wang, H.; Li, B.; Hou, G.; Yin, Z.; Wu, L.; Yam, V. W. *Angew. Chem., Int. Ed.* **2010**, *49*, 9233. (k) Chen, S.; Chen, L.-J.; Yang, H.-B.; Tian, H.; Zhu, W. *J. Am. Chem. Soc.* **2012**, *134*, 13596. (l) Lu, X.; Guo, Z.; Sun, C.; Tian, H.; Zhu, W. *J. Phys. Chem. B* **2011**, *115*, 10871. (m) Percec, V.; Dulcey, A. E.; Balagurusamy, V. S. K.; Miura, Y.; Smidrkal, J.; Peterca, M.; Nummelin, S.; Edlund, U.; Hudson, S. D.; Heiney, P. A.; Duan, H.; Magonov, S. N.; Vinogradov, S. A. *Nature* **2004**, *430*, 764. (n) Rosen, B. M.; Peterca, M.; Morimitsu, K.; Dulcey, A. E.; Leowanawat, P.; Resmerita, A.-M.; Imam, M. R.; Percec, V. *J. Am. Chem. Soc.* **2011**, *133*, 5135. (o) Kaucher, M. S.;

Peterca, M.; Dulcey, A. E.; Kim, A. J.; Vinogradov, S. A.; Hammer, D. A.; Heiney, P. A.; Percec, V. *J. Am. Chem. Soc.* **2007**, *129*, 11698.

- (3) (a) Kim, Y.; Li, W.; Shin, S.; Lee, M. *Acc. Chem. Res.* **2013**, *46*, 2888. (b) Shin, S.; Lim, S.; Kim, Y.; Kim, T.; Choi, T.-L.; Lee, M. *J. Am. Chem. Soc.* **2013**, *135*, 2156. (c) Kim, Y.; Kim, T.; Lee, M. *Polym. Chem.* **2013**, *4*, 1300. (d) Huang, Z.; Lee, H.; Lee, E.; Kang, S.-K.; Nam, J.-M.; Lee, M. *Nat. Commun.* **2011**, *2*, 459. (e) Moon, K. S.; Kim, H. J.; Lee, E.; Lee, M. *Angew. Chem., Int. Ed.* **2007**, *46*, 6807. (f) Kim, H.-J.; Lee, J.-H.; Lee, M. *Angew. Chem., Int. Ed.* **2005**, *44*, 5810. (g) Lee, M.; Lee, S.-J.; Jiang, L.-H. *J. Am. Chem. Soc.* **2004**, *126*, 12724. (h) Kim, J.-K.; Lee, E.; Kim, M.-C.; Sim, E.; Lee, M. *J. Am. Chem. Soc.* **2009**, *131*, 17768. (i) Ryu, J.-H.; Lee, E.; Lim, Y.-b.; Lee, M. *J. Am. Chem. Soc.* **2007**, *129*, 4808. (j) Ryu, J.-H.; Lee, M. *J. Am. Chem. Soc.* **2005**, *127*, 14170. (k) Huang, Z.; Kang, S.-K.; Lee, M. *J. Mater. Chem.* **2011**, *21*, 15327. (l) Lee, E.; Kim, J. K.; Lee, M. *Macro. Rapid Commun.* **2010**, *31*, 975. (m) Lee, E.; Kim, J.-K.; Lee, M. *J. Am. Chem. Soc.* **2009**, *131*, 18242. (n) Lee, E.; Kim, J.; Lee, M. *Angew. Chem., Int. Ed.* **2008**, *47*, 6375. (o) Ryu, J.-H.; Kim, H.-J.; Huang, Z.; Lee, E.; Lee, M. *Angew. Chem., Int. Ed.* **2006**, *45*, 5304.
- (4) Kim, Y.; Shin, S.; Kim, T.; Lee, D.; Seok, C.; Lee, M. *Angew. Chem., Int. Ed.* **2013**, *52*, 6424.
- (5) Lee, E.; Kim, J.-K.; Lee, M. *Angew. Chem., Int. Ed.* **2009**, *48*, 3657.
- (6) (a) Kim, H.-J.; Kang, S.-K.; Lee, Y.-K.; Seok, C.; Lee, J.-K.; Zin, W.-C.; Lee, M. *Angew. Chem., Int. Ed.* **2010**, *122*, 8649. (b) Huang, Z.; Kang, S.-K.; Banno, M.; Yamaguchi, T.; Lee, D.; Seok, C.; Yashima, E.; Lee, M. *Science* **2012**, *337*, 1521.
- (7) (a) Huang, J.; Heise, A. *Chem. Soc. Rev.* **2013**, *42*, 7373. (b) Huang, Z.; Kang, S.-K.; Lee, M. *J. Mater. Chem.* **2011**, *21*, 15327. (c) Yan, X.; Wang, F.; Zheng, B.; Huang, F. *Chem. Soc. Rev.* **2012**, *41*, 6042.
- (8) (a) Ortony, J. H.; Newcomb, C. J.; Matson, J. B.; Palmer, L. C.; Doan, P. E.; Hoffman, B. M.; Stupp, S. I. *Nat. Mater.* **2014**, *13*, 812. (b) Shao, H.; Nguyen, T.; Romano, N. C.; Modarelli, D. A.; Parquette, J. R. *J. Am. Chem. Soc.* **2009**, *131*, 16374.
- (9) (a) Kim, H.-J.; Kim, J.-K.; Lee, M. *Chem. Commun.* **2010**, *46*, 1458. (b) Kim, H.-J.; Liu, F.; Ryu, J.-H.; Kang, S.-K.; Zeng, X.; Ungar, G.; Lee, J.-K.; Zin, W.-C.; Lee, M. *J. Am. Chem. Soc.* **2012**, *134*, 13871. (c) Soininen, A. J.; Kasëmi, E.; Schlüter, A. D.; Ikkala, O.; Ruokolainen, J.; Mezzenga, R. *J. Am. Chem. Soc.* **2010**, *132*, 10882.
- (10) (a) Lee, D.-W.; Kim, T.; Park, L.-S.; Huang, Z.; Lee, M. *J. Am. Chem. Soc.* **2012**, *134*, 14722. (b) Lim, Y.; Moon, K. S.; Lee, M. *Angew. Chem., Int. Ed.* **2009**, *48*, 1601.
- (11) Rosen, B. M.; Wilson, C. J.; Wilson, D. A.; Peterca, M.; Imam, M. R.; Percec, V. *Chem. Rev.* **2009**, *109*, 6275.
- (12) (a) Kato, T.; Kihara, H.; Kumar, U.; Uryu, T.; Fréchet, J. M. J. *Angew. Chem., Int. Ed.* **1994**, *33*, 1644. (b) Lee, M.; Cho, B.-K.; Kang, Y.-S.; Zin, W.-C. *Macromolecules* **1999**, *32*, 8531. (c) Kato, T.; Mizoshita, N.; Kanie, K. *Macromol. Rapid Commun.* **2001**, *22*, 797.
- (13) Puranik, P. G.; Jaya Rao, A. M. *Proc. - Indian Acad. Sci., Sect. A* **1957**, *45*, 51.
- (14) (a) Chan, J. M.; Tischler, J. R.; Kooi, S. E.; Bulovic, V.; Swager, T. M. *J. Am. Chem. Soc.* **2009**, *131*, 5659. (b) Würthner, F.; Kaiser, T. E.; Saha-Möllner, C. R. *Angew. Chem., Int. Ed.* **2011**, *50*, 3376. (c) Ghosh, S.; Li, X. Q.; Stepanenko, V.; Würthner, F. *Chem.—Eur. J.* **2008**, *14*, 11343.
- (15) (a) Shao, H.; Seifert, J.; Romano, N. C.; Gao, M.; Helmus, J. J.; Jaroniec, C. P.; Modarelli, D. A.; Parquette, J. R. *Angew. Chem., Int. Ed.* **2010**, *49*, 7688. (b) Cheetham, A. G.; Zhang, P.; Lin, Y.-a.; Lock, L. L.; Cui, H. *J. Am. Chem. Soc.* **2013**, *135*, 2907. (c) Xu, H.; Das, A. K.; Horie, M.; Shaik, M. S.; Smith, A. M.; Luo, Y.; Lu, X.; Collins, R.; Liem, S. Y.; Song, A.; Popelier, P. L. A.; Turner, M. L.; Xiao, P.; Kinloch, I. A.; Ulijn, R. V. *Nanoscale* **2010**, *2*, 960.
- (16) (a) Rekharsky, M. V.; Mori, T.; Yang, C.; Ko, Y. H.; Selvapalam, N.; Kim, H.; Sobransingh, D.; Kaifer, A. E.; Liu, S.; Isaacs, L. *Proc. Natl. Acad. Sci. U.S.A.* **2007**, *104*, 20737. (b) Moghaddam, S.; Inoue, Y.; Gilson, M. K. *J. Am. Chem. Soc.* **2009**, *131*, 4012. (c) Ogoshi, T.; Kanai, S.; Fujinami, S.; Yamagishi, T.-a.; Nakamoto, Y. *J. Am. Chem. Soc.* **2008**, *130*, 5022.
- (17) Hernandez-Garcia, A.; Kraft, D. J.; Janssen, A. F. J.; Bomans, P. H. H.; Sommerdijk, N. A. J. M.; Thies-Wespie, D. M. E.; Favretto, M. E.; Brock, R.; de Wolf, F. A.; Wertén, M. W. T.; Schoot, P. v. d.; Stuart, M. C.; de Vries, R. *Nat. Nanotechnol.* **2014**, *9*, 698.